SOLID MATTER

YA.M. OLIKH, M.D. TYMOCHKO

V.E. Lashkaryov Institute of Semiconductor Physics, Nat. Acad. of Sci. of Ukraine
(41, Prosp. Nauky, Kyiv 03028, Ukraine; e-mail: jaroluk3@ukr.net)

PACS 72.20.My, 72.80.Ey, 74.25.Ld

PECULIARITIES OF CURRENT FLOW IN STRONGLY COMPENSATED LOW-RESISTANCE CdTe:Cl CRYSTALS UNDER ULTRASONIC LOADING

To elucidate the mechanism of influence of ultrasound on the temperature, T, dependence of conductivity ($\sigma(T)$) in low-resistance CdTe:Cl ($N_{Cl} \approx 10^{24}$ m^{-3}) single crystals of the n-type, the Hall effect and the relaxation kinetics of $\sigma(t)$ at the ultrasound ($f_{US} \sim 10$ MHz, $W_{US} \sim 10^4$ W/m^2) switching-on and -off have been studied in a temperature interval from 77 to 300 K. A completely reversible dynamical influence of ultrasound is revealed for the first time. It has different characters for the low (LT, $T < 180$ K) and high (HT, $T > 200$ K) temperature intervals. Acoustically stimulated changes in the HT region are found to be insignificant: the mobility of charge carriers decreases a little, and long-term processes of $\sigma(t)$ relaxation are not observed. In the LT region, the relative acoustically stimulated changes grow; in particular, the duration of $\sigma(t)$ relaxation processes increases, and they reveal a two-stage character. To explain this phenomenon, the model of a heterogeneous semiconductor containing clusters of impurity defects in vicinities of dislocations is applied. A mechanism is proposed that relates the "instant" increase of $\sigma(t)$ with the acoustically stimulated reduction of the amplitude of fluctuations of the large-scale potential owing to the enlargement of the effective electronic radius of dislocation impurity clusters. Long-term (50–500 s) temperature-dependent relaxation processes are governed by the diffusive reconstruction of the point-defect structure in the cluster bulk, including the transformation of acceptor $(V_{Cd}^{2-} Cl_{Te}^{+})^{-}$ complexes into neutral $(V_{Cd}^{2-} 2Cl_{Te}^{+})^{0}$ ones.

K e y w o r d s: ultrasound, dislocations, CdTe single crystals, Hall effect, conductivity relaxation.

1. Introduction

Electrophysical, optical, and photo-electric parameters of semiconductors are known to be mainly governed by the impurity-defect structure of a crystal. Therefore, the control over the physical characteristics of those materials can be reached, by using a purposeful reorganization of this structure. The corresponding active external treatments include the thermal annealing, γ-irradiation, hydrogen treatment, microwave irradiation, ultrasonic treatment, and oth-

ers. Ultrasound turns out the simplest external factor from the above-mentioned ones. It can give rise to the transformation of impurity-defect complexes and can result in the corresponding residual modifications of electrophysical parameters [1–4]. The following A_2B_6 compounds are especially sensitive from this viewpoint with regard for a high concentration of dislocations in them ($N_{Dis} \sim 10^{10} m^{-2}$) and a high efficiency of acousto-dislocation interaction: CdS, ZnS, CdTe, ZnCdTe, and CdHgTe.

The basic model that can explain those modifications is the dislocation one. The propagation of an intensive ultrasound wave makes the dislocations vib-

rate. At the ultrasound intensity $W_{us} \sim 10^4$ W/m^{-2} and the dislocation concentration $N_{Dis} \sim 10^{10}$ m^{-2}, the acoustically stimulated (AS) reorganization of defects extends, in fact, over the whole specimen volume. It is considered that, under the action of an ultrasound wave, electrically active point defects are "captured" or "released" from dislocations, which serve as sinks for them, and a certain reconstruction of point-defect complexes in vicinities of dislocations takes place [5]. Depending on the state of the impurity-defect structure and the parameters of an ultrasound wave, the experiment can give rise to residual or temporary modifications, the latter being observed only in the course of ultrasound treatment. Earlier, only residual AS effects in CdTe crystals were studied [6].

Doped CdTe:Cl single crystals attract a high interest for a long time both in the practical aspect – the manufacture of uncooled X-ray and γ-radiation detectors for the environmental radiation monitoring [7, 8] – and as model specimens to study inhomogeneities in the defect structure of crystals [9] and the influence of related large-scale potential fluctuations on transfer phenomena [10], residual conductivity [11], long-term photoconductivity relaxation [12], and hopping conductivity [13, 14]. However, despite that the A_2B_6 compounds, including CdTe, are unique from the viewpoint of a very strong interaction between the electron and dislocation systems of the specimen (any modifications in either of them are immediately reflected as variations in the other [15–17]), the role of dislocations remained almost beyond the scope of discussion in the above-cited fundamental works [7–14] dealing with electrophysical and photoelectric properties of CdTe:Cl .

As was shown in many early works, the examined low-resistance CdTe:Cl specimens are characterized not only by a high dislocation concentration N_{Dis}, but also a variety of defect complexes containing the Cl impurity [11, 18]. At that, some of Cl atoms are located at the acceptor, $(V_{Cd}^{2-}Cl_{Te}^{+})^{-}$, and neutral, $(V_{Cd}^{2-}2Cl_{Te}^{+})^{0}$ and $(V_{Cd}^{-}Cl_{Te}^{+})^{0}$, complexes [7]. Some others are captured at the dangling bonds of dislocations. One may expect that such an involved impurity-defect system of the crystal can become rather labile under the ultrasound loading – in particular, owing to the AS growth of the diffusion coefficient for some point defects – already at low temperatures (<300 K).

This situation looks favorable for studying the dynamical (*in situ*) AS effects and makes it possible to preliminarily consider CdTe as a model substance for studying the acousto-dislocation-electron interaction in semiconductors. Really, the dynamical AS variations in the electrophysical parameters of CdTe:Cl, which were attributed to overcompensation effects, were revealed by us for the first time in work [19]. However, a complicated two-stage character of the acousto-conductivity relaxation in those specimens, when ultrasound was switched-on and -off, revealed new features of AS effects, in particular, under the hopping conductivity conditions, which earlier have not been analyzed in semiconducting substances at all.

The work was aimed at studying the basic characteristics of the influence of ultrasound on the current flow in strongly compensated dislocation CdTe:Cl specimens and at elucidating the role of dislocations in AS effects.

2. Experimental Specimens and Technique

Chlorine-doped cadmium telluride single crystals (CdTe:Cl) were fabricated, by using the vertical Bridgman method at a low cadmium vapor pressure in an ampoule [20]. The chlorine impurity concentration in the melt amounted to $N_{Cl}^0 \approx 10^{24}$ m^{-3}. The ohmic contacts on the specimens $2 \times 3 \times 8$ mm^3 in dimensions were formed, by using the thermal sputtering of indium in vacuum at a temperature of 175 °C. The concentration n and the mobility μ of charge carriers in a temperature interval of 77–300 K were determined, by using the Hall method in the regime of dc electric and magnetic fields. The electrophysical parameters under the ultrasound loading were measured (the acousto-Hall method) in a liquid-nitrogen cryostat equipped with acoustic elements. The cryostat construction allowed the measurements to be sequentially carried out for the same specimen with its impurity-defect system in different states, initial and acoustically perturbed ones [21]. The dynamical regime of the ultrasound action, i.e. when the reversible character of modifications was observed, made also it possible to systematically monitor the transient processes and the relaxation kinetics of the conductivity $\sigma(t)$. Such a capability turned out especially useful at short relaxation times in the pulse regime of acoustic loading [22].

A longitudinal ultrasound wave with a frequency of about 10 MHz and an intensity of up to 2×10^4 W/m^2 was introduced into the specimen through a dielectric buffer plate from a piezoelectric transducer, a $(Y + 36°)$-cut lithium niobate plate, fed with a sinusoidal signal obtained from a high-frequency generator (see the diagram of the acoustic unit in the inset in Fig. 1). The measurement accuracy of electric signals under the ultrasound loading was about 10^{-6} V, and that of temperature about 0.1 K. The specimen temperature variation under the intensive ultrasound loading in the course of the measurement of a separate experimental point did not exceed 2–3 K.

The same cryostat was used in the temperature interval $T = 79 \div 173$ K to study the relaxation dependences $\sigma(t)$ when the ultrasound loading was switched-on and -off. For this purpose, a digital multimeter UT71A was used. The temporal variations $\sigma(t)$ were measured with a step of about 1 s. In addition, they were visually monitored on a computer screen, making the control over a possible heating or cooling of the specimen. The corresponding oscillations δT varied from 0.1 to 5 K at that. Their time behavior was registered for every relaxation dependence and, afterwards, were taken into account as corrections when calculating $\sigma(t)$.

3. Results

We found that the observed AS changes of the Hall coefficient R_{H} and the conductivity σ are reversible. When ultrasound was switched-on, and the acoustic action terminated, the specimen parameters slowly (50–500 s, depending on the temperature and the ultrasound intensity) returned to their initial values that they had before the ultrasound treatment. Figures 1, 2, 4, and 5 demonstrate the values of relaxed (stable) parameter.

3.1. Temperature dependences of conductivity $\sigma(T)$

Figure 1 shows the temperature dependences of σ for the initial specimen (without ultrasound loading, curve *1*) and the specimen under the ultrasound action (curve *2*). In the latter case, σ changes: weakly at room temperature. However, if the temperature is lowered, the relative modifications reach 30%. From Fig. 1, one can see that the examined temperature interval can be divided into two sections, in which the characters of temperature-induced and, especially, AS
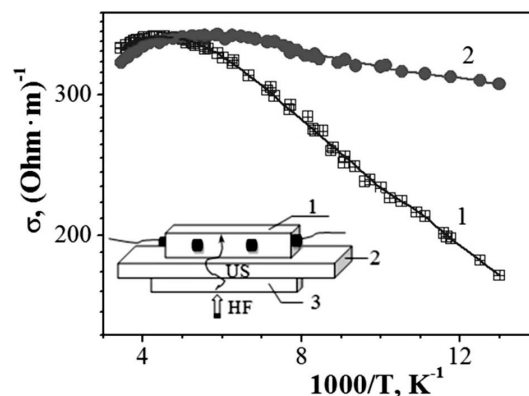

Fig. 1. Temperature dependences of the conductivity $\sigma(T)$ in CdTe:Cl: (1) without ultrasound and (2) under ultrasound loading ($W_{\mathrm{US}} \approx 2 \times 10^4$ W/m^2). In all figures, curves with hollow symbols (or marked by "1" or "0") correspond to initial specimens, and curves with solid symbols (or marked by "2" or "us") to the ultrasound loading. The inset demonstrates the scheme of an acoustical unit: specimen (*1*), buffer (*2*), piezoelectric transducers (*3*), high frequency (HF), ultrasound (US)

changes in $\sigma(T)$ are qualitatively different. These are the high-temperature (HT, $T > 200$ K) and low-temperature (LT, $T < 180$ K) intervals.

3.2. Temperature dependences of charge carrier mobility

In order to understand the mechanism of change of a conductivity under the ultrasound loading, it is very important to distinguish AS modifications associated with the variations in the concentration and the mobility of charge carriers. This task can be done taking advantage of Hall effect measurements. Supposing our specimens to be homogeneous, we formally calculated $\mu_{\mathrm{H}} = R_{\mathrm{H}}\sigma$ and $n_e = (eR_{\mathrm{H}})^{-1}$, by using the standard method. In Fig. 2, the temperature dependences of the electron mobility, $\mu_{\mathrm{H}}(T)$, are depicted for the cases of ultrasound absence (curve *1*) and loading (curve *2*).

From Fig. 2, one can see that the propagation of an ultrasound wave in the crystal substantially affects the dependence $\mu_{\mathrm{H}}^{\mathrm{US}}(T)$. In the HT interval, the character of $\mu_{\mathrm{H}}^{\mathrm{US}}(T)$ does not change. Only some reduction of the $\mu_{\mathrm{H}}^{\mathrm{US}}(T)$ magnitude is observed. On the contrary, in the LT interval, the ultrasound action gives rise to a considerable increase of the $\mu_{\mathrm{H}}^{\mathrm{US}}(T)$ magnitude, which becomes practically independent of the temperature. According to the theory, those two distinct temperature sections in the $\mu_{\mathrm{H}}(T)$ de-
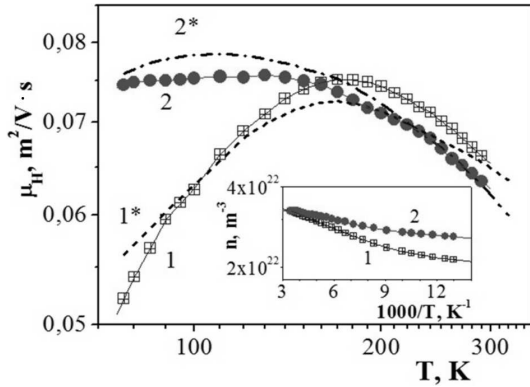
Fig. 2. Temperature dependences of charge carrier mobilities in CdTe:Cl: (*1* and *1**) without ultrasound, (*2* and *2**) under the ultrasound loading ($W_{US} \approx 2 \times 10^4$ W/m^2). Symbols correspond to experimental data, and curves to the calculation results. The inset demonstrates the temperature dependences of the electron concentration: without ultrasound (*1*), under the ultrasound loading (*2*)

pendence for the initial specimen correspond, generally speaking, to the basic mechanisms of charge carrier scattering in semiconductors [24]. The scattering by ionized impurities dominates in the LT section, and the scattering by thermal vibrations of the crystal lattice prevails at temperatures close to room one. Making allowance for those two scattering mechanisms, we managed to satisfactorily describe the experimental data obtained for $\mu_H(T)$ (theoretical curve *1** in Fig. 2). The best correspondance between the experimental (*1*) and calculated (*1**) curves was achieved for the values $n \approx 2.3 \times 10^{22}$ m^{-3} (see the inset in Fig. 2) and $N_{II}^0 \approx 7.6 \times 10^{23}$ m^{-3} (N_{II} is the concentration of ionized impurities in the Brooks–Herring model). Curve *2* in Fig. 2 was obtained at the ultrasound loading. In order to put the calculated curve *2** in a satisfactory agreement with the experimental dependence 2 in the HT interval ($T > 200$ K), we calculated $\mu_H^{US}(T)$ by *formally including* additional scattering at acoustic phonons ($\mu_{ph} = AT^{-0.5}$, where A is a certain effective coefficient, which practically does not depend on the temperature and is to be fitted). This trick allowed us to obtain acceptable agreement between calculated curve *2** and experimental dependence 2. Note that the accurate calculation of the coefficient A in the case of the acoustically perturbed phonon system of a crystal is impossible. In the LT interval ($T < 150$ K), the scattering by ionized impurities

dominates in the case of ultrasound application as well. The corresponding fitted value for the concentration of scattering centers amounted to $N_{II}^{US} \approx$ $\approx 5.0 \times 10^{23}$ m^{-3}.

The inset in Fig. 2 demonstrates the temperature dependence of the electron concentration $n_e(T)$ calculated on the basis of the experimental dependence of the Hall coefficient $R_H(T)$. Here, curve *1* corresponds to the initial parameters of the crystal, i.e. without the ultrasound action. Under the ultrasound loading (curve *2*), the electron concentration increases. This parameter changes insignificantly at room temperature, but as the temperature decreases to liquid-nitrogen ones, its AS modification achieves about 20%. Note that the dependences $n(T)$ are monotonic in the whole interval of measurements for both the initial specimen and the specimen under the ultrasound loading, although the dependences are weak. According to the theory of semiconductors, this type of the $n(T)$-dependence is characteristic of the temperatures, at which the impurity donor level is exhausted, because it is the ionization of this level that governs the concentration of free electrons in the conduction band [24].

We also attract attention to the values of experimental mobility measured at high temperatures (600–650 cm^2/V/s). They are lower in comparison with tabulated ones for perfect crystals (1000–1200 cm^2/V/s [23]). This fact testifies to a high inhomogeneity of the specimen [9].

3.3. Conductivity relaxation at the ultrasound switching-on and -off

In Fig. 3, the temperature dependences of the conductivity $\sigma_i(T)$ in the HT interval at definite relaxation stages after the ultrasound switching-on (panel *a*) and -off (panel *b*) are depicted. The insets demonstrate the characteristic variations of σ in time at the temperature $T \approx 121$ K.

A detailed analysis of those dependences testify that the AS relaxation $\sigma(t)$, in general, is not monotonic, but runs at least in two stages. Really, at the time moment, when ultrasound is switched-on (off), an "instant" jump-like variation of σ takes place. Later, it transforms into a long-term monotonic relaxation. The estimation of the first stage brings about the value $\tau_1 < 1.0$ s. The kinetics of this stage was not studied in more details, because such small time intervals were shorter than the time resolution of

the digital part of our measurement installation. At the same time, the duration of the second stage τ_2 amounted to 50–500 s. The total duration of relaxation, which increased a little as the specimen temperature decreased, testifies to long-term mechanisms of AS reconstruction in the impurity-defect system of the crystal. Moreover, as was already mentioned above, even a long (for hours and longer) ultrasound loading of the specimen at chosen ultrasound regimes did not give rise to residual changes in the crystal parameters.

Note that the revealed AS relaxation of the conductivity in CdTe:Cl is similar to the long-term relaxation of the photoconductivity in inhomogeneous semiconductors [25]. We also attract attention to the fact that the relaxation times at the ultrasound switching-on and -off differ from each other by a factor of about two (see the insets in Fig. 3). This difference testifies not only to the diffusion character of the reorganization in the point-defect system, but also to the influence of ultrasound on this process. At the same time, the complete reproduction of relaxation curves obtained at repeated ultrasound switchings-on and -off at a fixed temperature confirms the stability of the dislocation structure as a whole.

In Fig. 3, the σ_0- and $\sigma_{\rm US}$-curves correspond to the beginning of the first switching stage, the $\sigma_{\rm US}^1$- and σ_0^1-ones to the end of the first stage, and $\sigma_{\rm US}^{\rm sat}$- and $\sigma_0^{\rm sat}$-ones to the end of the second stage. The straightening of the dependences $\sigma_i(T)$ in the coordinates $\ln \sigma$ versus T^{-1} may testify to the thermal activation of AS variations; in other words, σ_i is formally described by the dependence $\sigma_i = \sigma_i^0 \exp(-\varepsilon_i/kT)$. From Fig. 3, one can see that the rate of temperature variations for the long-term components of the AS conductivity growth/reduction, $\sigma_{\rm US}^{\rm sat} - \sigma_{\rm US}^1$, is about seven times as high as that for the "instant" change $\sigma_{\rm US}^1 - \sigma_0$. This fact convincingly testifies to different mechanisms of ultrasound action giving rise to the "instant" (jump-like) and long-term AS changes.

3.4. Dislocation parameters of examined specimens

The X-ray topographical method was applied to study the large face of a CdTe:Cl specimen, through which the ultrasound wave was introduced into the crystal. The analysis of reflections [220] and [440] from this plane, which had the (110) orientation, on
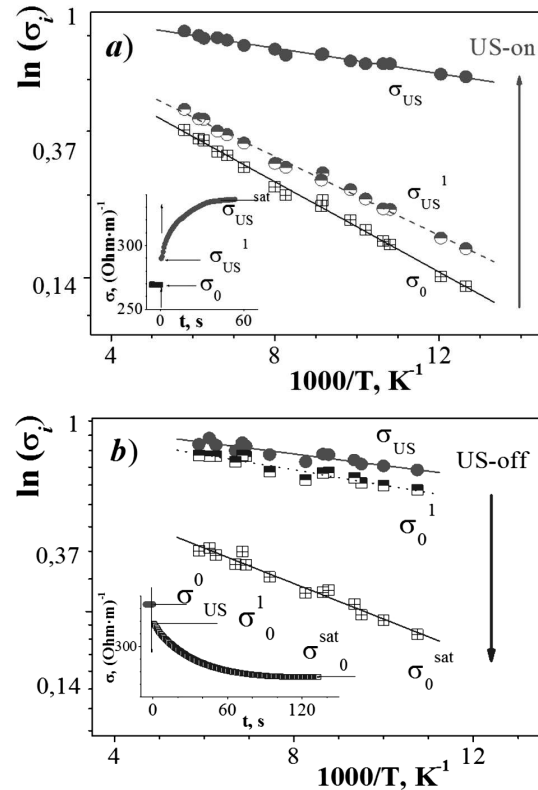

Fig. 3. Temperature dependences of conductivities $\sigma_i(T)$ in CdTe:Cl at certain relaxation stages after the ultrasound ($W_{\rm US} \approx 2 \times 10^4$ W/m^2) switching-on (*a*) and -off (*b*). Curves designated by σ_0 and $\sigma_{\rm US}$ correspond to the beginning of the switching; curves σ_0^1 and $\sigma_{\rm US}^1$ to the end of the first stage, and curves $\sigma_0^{\rm sat}$ and $\sigma_{\rm US}^{\rm sat}$ to the end of the second stage. The insets illustrate typical $\sigma(t)$-oscillograms obtained at $T \approx 121$ K, in which selected reference time marks σ_i are indicated

the basis of the Williamson–Hall technique [26] allowed us to preliminarily estimate the state of the specimen crystal lattice. The concentration of screw dislocations was found to equal $N_{\rm Dis}^{XR} \approx 5 \times 10^{12}$ m^{-2}, and the lattice strain $\varepsilon_L^{XR} \approx 5 \times 10^{-5}$.

3.5. Recapitulation of typical experimental regularities

3.5.1. Low mobility values are observed at room temperature, which unambiguously confirms a considerable contribution made by crystal inhomogeneities that are associated with impurity clusters in CdTe:Cl [9,10] to the charge carrier scattering. This conclusion is supported by a steep (steeper that $T^{3/2}$) temperature dependence of $\mu_{\rm H}$ at $T < 100$ K [27,28].

3.5.2. Proceeding from the experimentally established character of AS changes in the electrophysical parameters, the studied temperature interval has to be considered separately: the low-temperature (LT) region at $T < 180$ K and the high-temperature (HT) one at $T > 200$ K. In the HT interval, the AS changes are insignificant: the mobility of charge carriers is a little lower, and the long-term relaxation of acousto-conductivity does not manifest itself. In the LT regions, when approaching liquid-nitrogen temperatures, the relative AS changes grow, and the duration of relaxation processes increases.

3.5.3. A two-stage character of the AS $\sigma(t)$-relaxation at low temperatures was revealed: this is an "instant" jump at the moment of the ultrasound switching followed by a monotonic long-term relaxation. This behavior testifies to the coexistence of several (two) processes (mechanisms) of ultrasound action. The considerably different rates for the temperature variations at the long-term and "instant" stages confirm that the mechanisms of corresponding AS changes are different.

3.5.4. The state of a dislocation structure in the specimen was determined. In particular, the high concentration of dislocations, $N_{\text{Dis}}^{XR} \approx 5 \times 10^{12}$ m^{-2}, and, accordingly, the substantial internal stretching strain in the lattice, $\varepsilon_L^{XR} \approx 5 \times 10^{-5}$, can be regarded as crucial for the main mechanism of ultrasound action to be realized.

3.5.5. Hence, the experimentally found regularities in the current flow and the specific features of the AS influence demand that a more thorough analysis concerning the features of a charge carrier motion in examined CdTe:Cl specimens should be done in comparison with that performed in Section 3.2, because the conditions of the current flow are also responsible for the mechanism of AS changes.

4. Discussion

4.1. General character of the current flow in the initial specimen

The main AS effects are observed in CdTe:Cl at low temperatures, and their amplitude increases with the temperature reduction. To understand the origin of the ultrasound action, it is necessary, first of all, on the basis of conclusions made in Section 3.5, to elucidate the mechanisms governing the current flow in the

initial specimen in detail. For this purpose, let us analyze information on the electrophysical parameters of the crystal. On the basis of experimental results on the Hall effect and the formal quantitative calculations (see Section 3.2), we found that, for the initial specimen, $N_I^0 = N_d + N_a \approx 7.6 \times 10^{23}$ m^{-3} and $n_e = N_d - N_a \approx 2.3 \times 10^{22}$ m^{-3}. Accordingly, the concentration of donors $N_d \approx 3.9 \times 10^{23}$ m^{-3}, that of acceptor centers $N_a \approx 3.7 \times 10^{23}$ m^{-3}, and the compensation degree $K_0 = N_a/N_d \approx 0.94$. The results of a similar calculation for the case of ultrasound loading look like $N_I^{\text{US}} \approx 5.0 \times 10^{23}$ m^{-3} and $n_e^{\text{US}} \approx 2.8 \times 10^{22}$ m^{-3}; accordingly, $N_d^{\text{us}} \approx 2.64 \times 10^{23}$ m^{-3}, $N_a^{\text{us}} \approx 2.36 \times 10^{23}$ m^{-3}, and $K_{\text{us}} \approx 0.89$.

We emphasize that the applicability of the standard calculation procedure to the determination of electrophysical parameters in our specimens using the Hall method in the whole temperature interval requires the additional discussion. However, for preliminary estimations at the qualitative level, we consider it to be correct. This is the more so because, as is shown below, the intensive ultrasound loading substantially weakens the influence of inhomogeneities and makes the conditions of a current flow in the specimen more similar to the homogeneous case.

Hence, as was marked in Section 3.5, the crystal structure inhomogeneity can be crucial for the processes of charge transfer and the effects of the ultrasound action in CdTe:Cl. The crystal structure of researched specimens was characterized by fluctuations of a potential relief, which emerged owing to the technological features of the production of this material [18, 20]. In particular, at the annealing of a crystal with a preliminarily high concentration of nonequilibrium intrinsic defects, the latter diffuse to the sinks and stimulate impurity atoms to migrate to those regions as well. The growth of the defect concentration around sinks is accompanied by an enhancement of the complex formation, which results, in turn, in an additional compensation and the semiconductor inhomogeneity growth. On the basis of the results of X-ray topography (see Section 3.4), the main sinks for point defects in our specimens are dislocations [15–17]. The high concentration of the doping impurity ($N_{\text{Cl}} \approx 10^{24}$ m^{-3}) favored the formation of point-defect clusters (Cottrell clouds) – first of all, around dislocations – even at the annealing stage. Hence, in such strongly compensated semiconductors (in our case, $K \approx 0.94$), the impurity band can play an important

role in the current flow processes [24, 29, 30]. In particular, if an electric field is applied to the specimen, there arises a complicated situation in it: two parallel channels of conductivity – free electrons in the conduction band and localized electrons in the impurity one – coexist simultaneously.

Therefore, first, the presence of clusters and the fluctuation potential gives rise to an additional (extra) scattering of charge carriers, including those in the conduction band. Second, under certain conditions (low temperatures), electrons that are localized at local impurity levels can, generally speaking, demonstrate the hopping conductivity both between the impurity atoms and between the defect clusters [24, 29, 30]. In this case, if the temperature decreases, the contribution of hopping conductivity grows (see Section 4.3 for more details). In this connection, a necessity in the introduction of two temperature intervals, which are conditionally separated (see Fig. 4) by a certain temperature $T_{\mathrm{fp}} \approx 159$ K ($\gamma_{\mathrm{fp}} = kT_{\mathrm{fp}} \approx 0.014$ eV), becomes clear. In particular, σ_{cb} prevails at $T > T_{\mathrm{fp}}$, whereas σ_{hc} may reveal itself at $T < T_{\mathrm{fp}}$.

In work [30], in the case where the band and hopping conductivity channels coexist, a formula was given for the calculation of the amplitude of root-mean-square fluctuations of the electrostatic potential for a conduction electron and an ionized donor. This formula allows the effective amplitude of potential relief fluctuations to be estimated:

$$W_p = \frac{1.64e^2}{4\pi\chi} \sqrt[3]{\frac{4\pi}{3}(n_e + N_{\mathrm{d}} + N_{\mathrm{a}})}. \qquad (1)$$

Substituting the data for our initial specimens ($N_{\mathrm{d}} \approx 3.9 \times 10^{23}$ m^{-3}, $N_{\mathrm{a}} \approx 3.7 \times 10^{23}$ n^{-3}, $n \approx 3 \times 10^{22}$ m^{-3}, and the dielectric constant $\chi = 12$) into Eq. (1), we obtain $W_p \approx 0.03$ eV.

4.2. Peculiarities of a current flow under the ultrasound loading: high-temperature interval

From Fig. 2, one can see that the ultrasound action does not change the character of the dependence $\mu_{\mathrm{H}}^{\mathrm{US}}(T)$; only some reduction of its magnitude is observed. The plotted dependence of the acoustically stimulated growth of the reciprocal mobility $\Delta(\mu_{\mathrm{H}})^{-1} = (\mu_{\mathrm{H}}^{\mathrm{US}})^{-1} - (\mu_{\mathrm{H}}^0)^{-1}$ on the temperature (see Fig. 4) demonstrates that $\Delta(\mu_{\mathrm{H}})^{-1} \approx 0.61$ V·s/m^2 in
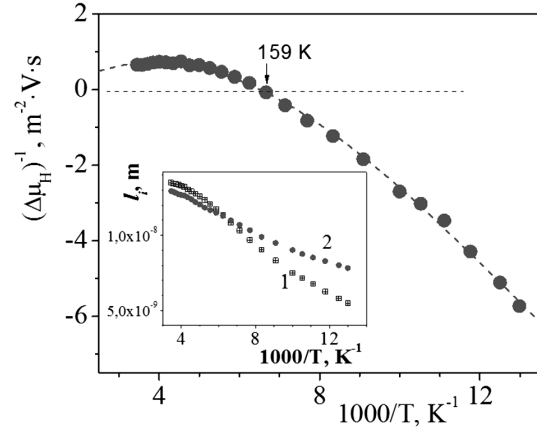

Fig. 4. Temperature dependences of the acoustically ($W_{\mathrm{US}} \approx \approx 2 \times 10^4$ W/m^2) induced growth of the mobility $\Delta(\mu_{\mathrm{H}})^{-1} = = (\mu_{\mathrm{H}}^{\mathrm{US}})^{-1} - (\mu_{\mathrm{H}}^0)^{-1}$ in CdTe:Cl. The inset demonstrates the temperature dependences of the electron mean free path: without ultrasound (*1*) and under the ultrasound loading (*2*)

the whole HT interval, i.e. the acoustic component of the AS scattering is almost independent of the temperature. Bearing in mind that the dislocation mechanism of interaction dominates for ultrasound waves in A_2B_6 crystals (see Introduction), it is reasonable to assume that the contribution to $\Delta(\mu_{\mathrm{H}})^{-1}$ is connected with the additional scattering of charge carriers in the conduction band of CdTe:Cl at dislocations that vibrate in the ultrasound field [24]:

$$\mu_{\mathrm{Dis}} = \frac{e}{m^*} \frac{3}{8v_T R_{\mathrm{Dis}} N_{\mathrm{Dis}}}, \qquad (2)$$

where e, m^*, and v_T are the charge, effective mass, and thermal velocity of an electron, respectively; R_{Dis} and N_{Dis} are the radius of the space charge of dislocations (the radius of Read cylinders) and their concentration, respectively.

For further calculations, let us evaluate theoretically the value of R_{Dis}^T for the stationary state (without ultrasound loading) by the formula [16]

$$R_{\mathrm{Dis}}^T = \sqrt{\frac{f}{\pi a N_{\mathrm{d}}}}. \qquad (3)$$

Here, a is the lattice period, $f \approx 0.1$ is the coefficient of dislocation filling by electrons [31], and $N_{\mathrm{d}} \approx 3.9 \times 10^{23}$ m^{-3}. From Eq. (3), we find that $R_{\mathrm{Dis}}^T \approx 1.1 \times 10^{-8}$ m. Now, by equating $\Delta(\mu_{\mathrm{H}}) = \mu_{\mathrm{Dis}}^{\mathrm{exp}}$ and taking into account that $R_{\mathrm{Dis}} = R_{\mathrm{Dis}}^T$, we use Eq. (2) to evaluate the concentration $N_{\mathrm{Dis}}^{\mathrm{eff}}$ that is
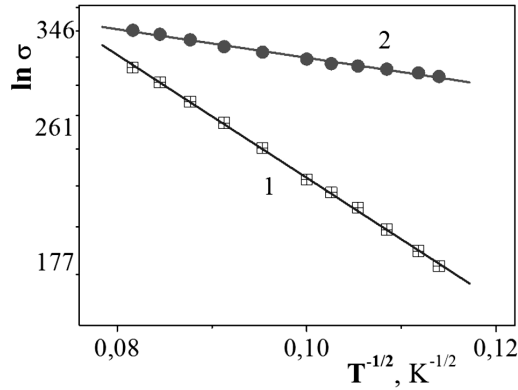
Fig. 5. Temperature dependences of the conductivity in CdTe:Cl: (without ultrasound *1*) and under the ultrasound loading ($W_{US} \approx 2 \times 10^4$ W/m^2) (*2*). Symbols correspond to experimental data, and lines to their approximations

required to explain the observed AS increase of the electron scattering in the HT interval:

$$N_{\mathrm{Dis}}^{\mathrm{eff}} = \frac{e}{m^*} \frac{3}{8v_T R_{\mathrm{Dis}} \Delta(\mu_{\mathrm{H}})}. \qquad (2^*)$$

Substituting $m^* = 0.1 m_e$, $v_{300} = 2.1 \times 10^5$ m/s, $\Delta \mu_{\mathrm{H}} = 1.6$ m^2/(V·s), and $R_{\mathrm{Dis}} \approx R_{\mathrm{Dis}}^T \approx 1.1 \times 10^{-8}$ m into this formula, we obtain $N_{\mathrm{Dis}}^{\mathrm{eff}} \approx 10^{14}$ m^{-2}. It is worth noting that this value looks too large for our specimens even in comparison with the data of X-ray researches, $N_{\mathrm{Dis}}^{XR} \approx 5 \times 10^{12}$ m^{-2}. This mismatch may stem from (i) the erroneous assumption about the additional electron scattering by dislocations that vibrate in the ultrasound field or (ii) the incorrectly calculated R_{Dis}^T-value.

Let us look into this discrepancy by applying relation (2) once more in the following form:

$$R_{\mathrm{Dis}}^{\mathrm{eff}} = \frac{e}{m^*} \frac{3}{8v_T N_{\mathrm{Dis}} \Delta(\mu_{\mathrm{H}})}. \qquad (2^{**})$$

Substituting $N_{\mathrm{Dis}} = N_{\mathrm{Dis}}^{XR} \approx 5 \times 10^{12}$ m^{-2}, we obtain $R_{\mathrm{Dis}}^{\mathrm{eff}} \approx 2.2 \times 10^{-7}$ m. One can see that this $R_{\mathrm{Dis}}^{\mathrm{eff}}$-value is about 20 times as large as the stationary theoretical value R_{Dis}^T. In our opinion, this result, in principle, is an illustration of a real situation, being very important for the understanding of the main mechanism of ultrasound action. Namely, it is quite feasible that the quantity $R_{\mathrm{Dis}}^{\mathrm{eff}}$ does not simply correspond to the Read radius of separate dislocations; instead, it evaluates the electronic radius of those space charge

regions, which give contribution to the charge carrier scattering. In other words, this is the effective radius of clusters composed of impurity atoms and intrinsic defects that are located around dislocations and, when the latter vibrate, become engaged into this process. Below, this value, $R_{\mathrm{Dis}}^{\mathrm{eff}} \approx 2.2 \times 10^{-7}$ m, will be roughly considered as the characteristic size of a dislocation cluster in the ultrasound field.

In order to understand the expected influence of ultrasound on the current flow at the qualitative level, let us estimate what fraction of the specimen volume can be occupied by such inhomogeneous space charge regions under the ultrasound loading. The corresponding value $\pi (R_{\mathrm{Dis}}^{\mathrm{eff}})^2 N_{\mathrm{Dis}} \approx 0.2$. In other words, inhomogeneities occupy 20% of the transverse specimen cross-section, and the other 80% belongs to the homogeneous specimen part. The evaluation was made for room temperature. At lower temperatures, v_T decreases, $v_T \sim (T)^{1/2}$, so that the volume fraction of clusters grows, and, already at 100 K, inhomogeneities occupy about 60% rather that 20% of the specimen volume.

4.3. Peculiarities of a current flow under the ultrasound loading: low-temperature interval

4.3.1. Mechanism of "hopping" conductivity

On the basis of the analysis concerning the coexistence of two parallel conductivity channels in our CdTe:Cl specimens (see Section 4.1), let us analyze the probability of a hopping conductivity between the defect clusters. In Fig. 5, the low-temperature ($T < 180$ K) experimental dependences of the conductivity are depicted in the coordinates $\ln \sigma$ versus $T^{-1/2}$ according to the Efros–Shklovskii law, which describes the tunneling of charge carriers over large distances [24, 29].

For quantitative estimations, we use the relation

$$\sigma_{\mathrm{hc}}^i = \sigma_i^0 \exp(-T_1^i/T)^{1/2}, \qquad (4)$$

where

$$T_1 = \beta_1 \frac{e^2}{k \varkappa a_{\mathrm{f}}}, \qquad (5)$$

the parameters σ_i^0 are determined from the experiment, the coefficient $\beta_1 = 2.8$, $\varkappa = 12$, k the Boltzmann constant, e the elementary charge, and a_{f} the localization radius for the states at the Fermi level

[13, 29]. From Fig. 5, one can see that the curves $\sigma_{\mathrm{hc}}^i(T)$ become undoubtedly straightened in the coordinates $\ln \sigma$ versus $T^{-1/2}$. The slope of those curves was used to determine T_1^i. Then, by applying formula (5), we calculated the radius $a_{\mathrm{f}} = \frac{\beta_1 e^2}{\varkappa k T_1}$ and a certain activation energy $\Delta_i^\sigma = k T_1^i$, which formally characterizes the hopping conductivity. The corresponding parameter values are quoted in Table. Hence, we obtained a result that is important for the understanding of the mechanism of ultrasound action: the estimate for a_{f} and for its AS growth (by almost a factor of 19), which corresponds to the AS reduction of $\Delta_{\mathrm{hc}}^{\mathrm{US}}$ to 1.5 meV.

The experimental data do not allow the contribution $\sigma_{\mathrm{hc}}^i(T)$ to be extracted separately. Therefore, we have no ground to talk about the absolute quantitative characteristics of the hopping conductivity, in particular, to interpret Δ_{hc}^i as the activation energy of the hopping conductivity. However, the character of the relative AS changes of the ratios $\Delta_{\mathrm{hc}}^{\mathrm{US}}/\Delta_{\mathrm{hc}}^0$ and $a_{\mathrm{f}}^{\mathrm{US}}/a_{\mathrm{f}}^0$ (their reduction) unambiguously testifies to a considerable weakening of the influence of inhomogeneities at the ultrasound loading. It is of interest that the coefficient for the AS growth of the state localization radius, $a_{\mathrm{f}}^{\mathrm{US}}/a_{\mathrm{f}}^0 \approx 19$, which was obtained from the LT $\sigma^i(T)$-dependences, correlates well with the coefficient for the AS growth of the effective electronic radius of clusters, $R_{\mathrm{Dis}}^{\mathrm{eff}}/R_{\mathrm{Dis}}^T \approx 20$, calculated from independent measurements of $\mu_{\mathrm{H}}^i(T)$ at high temperatures (see Section 4.2). This coincidence enhances the correctness of our qualitative assumptions and the following quantitative calculations. Another correlation – between $\Delta_{\mathrm{hc}}^i \approx 0.028$ eV and the amplitude of electrostatic potential fluctuations $W_p \approx 0.03$ eV, which were also obtained independently – has to be mentioned as well.

4.3.2. Analysis of mechanisms of electron scattering by inhomogeneities

While analyzing possible mechanisms in specific experimental situations, the ratio between the electron mean free path l_e and the inhomogeneity size A may be important [24]. The inset in Fig. 4 demonstrates the temperature dependences of l_e^i calculated by the formula
$$l_e^i = v_T \frac{m^*}{e} \mu_{\mathrm{H}}^i. \tag{6}$$
One can see that, for CdTe:Cl in the interval $T = 300 \div 100$ K, we have $l_e^i = (0.14 \div 0.08) \times 10^{-7}$ m,

and this value weakly depends on the temperature. As a value for the inhomogeneity size A, let us take the estimate for the radius of a dislocation cluster, $R_{\mathrm{Dis}} = (0.11 \div 2.2) \times 10^{-7}$ m, which was made above on the basis of experimental data, and the localization radius for states at the Fermi level, $a_{\mathrm{f}} = (1.5 \div 28) \times 10^{-7}$ m for the initial specimen and under the ultrasound loading (see Table).

a. Scattering at small-scale inhomogeneities. This situation can arise, when $l_e > A$. Then the scattering can be considered in the framework of the Weisberg model [27], in which $\mu_{\mathrm{H}} \sim T^{-5/6}$. Really, if we suppose that $A \approx R_{\mathrm{Dis}}$ in the initial specimen, then $l_e \approx A$, and this mechanism can be partially realized at high temperatures. Under the ultrasound loading, owing to the AS growth of the effective (for the charge carrier scattering) size of cluster regions, the Weisberg mechanism of scattering becomes inefficient, so that there emerges an opportunity of a certain AS growth for μ_{H}.

b. Scattering at large-scale inhomogeneities ($l_e < A$). According to the results of calculations presented above, this is a situation that is mainly realized in our experiments. Provided that $l_e < A$, the potential created by inhomogeneities modulates the concentration of "internal" charge carriers (the tunneling of charge carriers through the barrier $W_p \approx 0.03$ eV) and practically does not give rise to the additional scattering of conduction electrons. Instead, it manifests itself as a certain effective (small) scattering potential Δ_μ^i. In this case, the drift mobility of charge carriers in the space between the clusters corresponds, in fact, to the value for a homogeneous specimen [24, 29]. As was shown in work [28], the value of Δ_μ^i can be estimated on the basis of experimental dependences $\mu_{\mathrm{H}}(T)$. Namely, supposing the Gaussian character for the distribution of this random potential, its calculation can be performed using the following relation:

$$\mu_{\mathrm{H}}^i = \mu_0^i \exp(-(\Delta_\mu^i)^2/2k^2T^2). \tag{7}$$

Parameters of hopping conductivity in CdTe:Cl

Specimen	T_1^i, K	a_{f}^i, m	Δ_{hc}^i, meV
Initial ($i = 0$)	319	1.5×10^{-7}	28
Under ultrasound ($i = \mathrm{US}$)	17.2	2.8×10^{-6}	1.5

Plotting our experimental results for $\mu_{\mathrm{H}}^0(T)$ and $\mu_{\mathrm{H}}^{\mathrm{US}}(T)$ in accordance with expression (7) – in the coordinates $\ln \mu_{\mathrm{H}}$ versus T^{-2}, those dependence become almost straightened – and measuring their slopes, we found that $\Delta_\mu^0 = 6.5$ meV and $\Delta_\mu^{\mathrm{US}} = 1.3$ meV. Hence, we obtained that $\Delta_\mu^i \leq kT$ in the whole LT interval and decreases under the ultrasound loading of the specimen. Therefore, the effects of electron scattering can be regarded as a major factor in the AS changes of $\sigma(T)$ and $\sigma(t)$.

c. Physical origins of a possible AS reduction of W_p potential.

– *AS increase of the charge carrier concentration* and the corresponding screening of collective barriers by free charge carriers [24]. In our case, this mechanism has a low probability because of an insignificant (only by a factor of about two) AS growth of the charge carrier concentration.

– *Variation of the compensation degree.* Really, a certain AS reduction of K (see Section 4.1) does take place and can result in a reduction of W_p, but it is also insignificant.

– *The AS increase of the electronic radius of a cluster.* Again, this is actually a principal reason. Really, in the spherical approximation, the fluctuation is characterized only by two parameters: the radius R_0 and the charge Q. Therefore, its potential equals $W_p = Q/(\chi R_0)$ [32]. The AS growth of any fluctuation (or cluster) size (according to our estimations, by a factor of about 20), provided that the charge of this fluctuation is constant at the earliest relaxation stages, means that the potential drops by the same factor.

4.3.3. Acousto-dislocation mechanism of changes of electrophysical parameters

Let us return to the role of dislocations under such complicated conditions for the current flow. It will be recalled that, in our ultrasound experiments, we have a situation where the translational motion and the AS generation of dislocations still do not take place. In the ultrasound field with $W_{\mathrm{us}} \approx 10^4$ W/m^2 and at the strain $\varepsilon_{\mathrm{us}} \approx 10^{-5}$, dislocations only vibrate, with the corresponding displacement being equal to $\xi^* \sim 100$ Å [33]. In this case, the vibrations of a charged dislocation may give rise to the electron exhaustion in the region of the Cottrell atmosphere, a weaker screening by neighbor ions, and the

capture of new charges from distant impurity centers [15–17]. Some of electrons can be transferred onto dislocation levels in the dislocation core; later, they can pass from the core into the conduction band. Those, now free, electrons participate in the charge transfer for some time, until they return to impurity centers, where they were captured from. Hence, the rearrangement of the equilibrium dislocation charge, when ultrasound is switched-on, includes the processes of electron exchange among the dislocation levels, the conduction band, and the energy levels of surrounding local centers [15].

In the case of reverse process after the ultrasound action has terminated, the charges of all "participants" in the charge redistribution, as well as their positions, have to be restored to their initial equilibrium states; just this situation is observed in our case. One may expect that the characteristic times of charge relaxation into the acoustically perturbed state and backward should coincide. In our experiments (see the insets in Fig. 3), the $\sigma(t)$-relaxation duration at the ultrasound switching-off was almost twice as large as at the switching-on. We consider this fact as a kind of additional confirmation that the reconstruction in the point-defect system has a diffusion character, and the diffusion coefficient grows in the ultrasound field [2, 34].

The AS increase of the size $R_{\mathrm{Dis}}^{\mathrm{eff}}$ of scattering regions, which was obtained in Section 4.1, can be associated with either their elastic AS growth at forced dislocation vibrations or the growth of the linear density of dislocation electric charge in the course of electron capture from impurity levels. When ultrasound is switched-on, the whole specimen volume, including the point-defect clusters that are mainly concentrated around dislocations, is brought within a short time interval of about 10^{-6} s into the vibrational motion with the frequency of an ultrasound wave. As a result, the value of $R_{\mathrm{Dis}}^{\mathrm{eff}}$ "instantly" grows up, and the redistribution of free charges takes place with the Maxwellian relaxation time. At the first stage, the total charge of an inhomogeneous region (the space charge region) remains constant; it only becomes redistributed over a much bigger volume. We may assume that, afterward as a result of new nonequilibrium states of the electric and deformation fields inside the cluster, there arise certain diffusion-driven motions of atoms both from the dislocation core to the complexes and backward. A long-term (compa-

rable with the long-term relaxation of conductivity) reorganization of complex centers takes place; for example, these are quasichemical transformation reactions of charged acceptor complexes $(V_{Cd}^{2-}Cl_{Te}^+)^-$ into neutral ones $(V_{Cd}^{2-}2Cl_{Te}^+)^0$ [7]. When the ultrasound loading is switched-off, the inverse process should be observed, because the probability of the $(V_{Cd}^{2-}Cl_{Te}^+)^-$ acceptor complex formation in the equilibrium state (without ultrasound) is much higher than that for the $(V_{Cd}^{2-}2Cl_{Te}^+)^0$ one [7].

A more detailed consideration of the mechanism of AS reorganization in the impurity-defect system demands additional researches.

5. Conclusions

In order to elucidate the mechanism of ultrasound action on the conductivity $\sigma(T)$ in low-resistance dislocation CdTe:Cl single crystals of the n-type ($N_{Cl} \approx 10^{24}$ m^{-3}), the temperature (77–300 K) researches of the Hall effect and the relaxation kinetics $\sigma(t)$ at the ultrasound ($f_{US} \sim 10$ MHz and $W_{US} \sim 10^4$ W/m^2) switching-on and -off were carried out. For the first time, the dynamical influence of ultrasound was revealed, which is qualitatively different in the LT ($T < 180$ K) and HT ($T > 200$ K) intervals. In the HT interval, the AS changes are insignificant: the charge carrier mobility becomes a little lower, and the long-term $\sigma(t)$-relaxation is not observed. In the LT interval, when approaching the liquid-nitrogen temperature, the relative AS changes grow, and the duration of relaxation processes $\sigma(t)$ becomes longer, with the latter revealing a two-stage character. For the explanation of those phenomena, the model of inhomogeneous semiconductor with clusters of impurity defects located around dislocations was used. A mechanism was proposed which connects the "instant" jumps in the $\sigma(t)$-dependence with the AS growth of the effective radius of dislocation clusters in the course of dislocation vibrations and with the interaction between dislocations and the electron system of the whole crystal. At the same time, the long-term temperature-dependent relaxation of the conductivity is associated with the diffusion-driven reconstruction of the point-defect structure in the cluster bulk, including the transformation of charged acceptor $(V_{Cd}^{2-}Cl_{Te}^+)^-$ complexes into neutral $(V_{Cd}^{2-}2Cl_{Te}^+)^0$ ones.

Our researches showed that underestimated μ_H^i-values can be explained by the fluctuations of the large-scale potential and the deep levels, the population of which depends on both the specimen temperature and the ultrasound intensity. Important from the practical veiwpoint is a conclusion that the intensive ultrasound loading considerably weakens the influence of inhomogeneities and makes the conditions of current flow in the specimen more similar to the homogeneous case.

1. I.V. Ostrovs'kyi and A.A. Korotchenkov. *Acoustooptics* (Vyshcha Shkola, Kyiv, 2003) (in Ukrainian).
2. S. Ostapenko, N.E. Korsunskaya, and M.K. Sheinkman, Solid State Phenom. **85–86**, 317 (2002).
3. O.Ya. Olikh, Ultrasonics **56**, 545 (2015).
4. Ya.M. Olikh and O.Ya. Olikh, Sensor. Elektron. Mikrosyst. Tekhnol. **1**, 19 (2004).
5. A.I. Vlasenko, Ya.M. Olikh, and R.K. Savkina, Fiz. Tekh. Poluprovodn. **33**, 410 (1999).
6. B.N. Babentsov, S.I. Gorban', I.Ya. Gorodetskii *et al.*, Fiz. Tekh. Poluprovodn. **25**, 1243 (1991).
7. D.V. Korbutyak, S.W. Mel'nychuk, E.V. Korbut, and M.M. Borysyk, *Cadmium Telluride: Impurity-Defect States and Detector Properties* (Ivan Fedorov, Kyiv, 2000) (in Ukrainian).
8. V.I. Khivrych, *Effects of Compensation and Ionizing Radiation in CdTe Single Crystals* (Institute for Nuclear Research, Kyiv, 2010) (in Ukrainian).
9. M.V. Alekseenko, E.N. Arkadyeva, and A.A. Matveev, Fiz. Tekh. Poluprovodn. **4**, 414 (1970).
10. N.V. Agrinskaya, E.N. Arkadyeva, and A.I. Terentyev, Fiz. Tekh. Poluprovodn. **23**, 231 (1989).
11. N.V. Agrinskaya, M.V. Alekseenko, E.N. Arkadyeva *et al.*, Fiz. Tekh. Poluprovodn. **9**, 320 (1975).
12. N.V. Agrinskaya and V.V. Shashkova, Fiz. Tekh. Poluprovodn. **24**, 697 (1990).
13. N.V. Agrinskaya and A.N. Alyoshin, Fiz. Tverd. Tela **31**, 277 (1989).
14. N.V. Agrinskaya and V.I. Kozub, Fiz. Tekh. Poluprovodn. **32**, 703 (1998).

15. *Electronic Properties of Dislocations in Semiconductors,* edited by Yu.A. Osipyan (Editorial URSS, Moscow, 2000) (in Russian).

16. V.B. Shikin and Yu.V. Shikina, Usp. Fiz. Nauk **165**, 887 (1995).

17. M. Reiche, M. Kittler, W. Erfurt *et al.*, J. Appl. Phys. **115**, 194303 (2014).

18. A.A. Matveev and A.I. Terentyev, Fiz. Tekh. Poluprovodn. **34**, 1316 (2000).

19. Ya.M. Olikh and N.D. Timochko, in *Proceedings of the 4th International Conference ISMART 2014* (Belorus. Gos. Univ. Publ. Center, Minsk, 2014), p. 112 (in Russian).

20. M.I. Ilashchuk, A.A. Parfenyuk, and K.S. Ulyanitskyi, Ukr. Fiz. Zh. **31**, 126 (1986).

21. Ya.M. Olikh and R.K. Savkina, Ukr. Fiz. Zh. **42**, 1385 (1997).

22. Ya.M. Olikh and M.D. Tymochko, Techn. Phys. Lett. **37**, 37 (2011).

23. *Physics of $A^{\mathrm{II}}B^{\mathrm{VI}}$ compounds,* edited by A.N. Georgobiani and M.K. Sheikman (Nauka, Moscow,1986) (in Russian).

24. V.L. Bonch-Bruevich and S.G. Kalashnikov, *Semiconductor Physics* (Nauka, Moscow, 1977) (in Russian).

25. M.K. Sheinkman and A.Ya. Shik, Fiz. Tekh. Poluprovodn. **10**, 209 (1976).

26. I.A. Gerko, V.I. Khrupa, V.P.Klad'ko, E.N. Kislovskii, and V.N. Merinov, Zavodsk. Laborat. **54**, 65 (1988).

27. L.R. Weisberg, J. Appl. Phys. **33**, 1817 (1962).

28. E.D. Golovkina, N.N. Levchenya, and A.Ya. Shik, Fiz. Tekh. Poluprovodn. **10**, 383 (1976).

29. B.I. Shklovskii and A.L. Efros, *Electronic Properties of Doped Semiconductors* (Springer, Berlin, 1984).

30. N.A. Poklonskii, *Ionization Equilibrium and Hopping Conductivity in Doped Semiconductors* (Belorus. Gos. Univ. Publ. House, Minsk, 2004) (in Russian).

31. M.M. Baran, I.M. Vas'kovych, Nauk. Visn. NLTU **22.15**, 336 (2012).

32. S.A. Omel'chenko, A.A. Gorban', M.F. Bulanyi, and A.A. Timofeev, Fiz. Tverd. Tela **48**, 830 (2006).

33. *Ultrasound. The Small Encyclopedia*, edited by I.P. Golyamina (Soviet Encyclopedia, Moscow, 1979) (in Russian).

34. V.N. Pavlovich, Phys. Status Solidi B **180**, 97 (1993).

Я.М. Оліх, М.Д. Тимочко

ОСОБЛИВОСТІ ПРОТІКАННЯ
СТРУМУ ПРИ УЛЬТРАЗВУКОВОМУ
НАВАНТАЖЕННІ В СИЛЬНО КОМПЕНСОВАНИХ
НИЗЬКООМНИХ КРИСТАЛАХ CdTe:Cl

Р е з ю м е

З метою виясненя механізму впливу ультразвуку (УЗ) на електропровідність $\sigma(T)$ у низькоомних монокристалах n-типу CdTe:Cl ($N_{\mathrm{Cl}} \approx 10^{24}$ м$^{-3}$) проведено температурні (77–300 K) дослідження ефекту Холла та кінетики релаксації $\sigma(t)$ при ввімкненні та вимкненні УЗ ($f_{\mathrm{US}} \sim 10$ МГц, $W_{\mathrm{US}} \sim 10^{4}$ Вт/м^2). Вперше виявлено динамічний (повністю зворотний) вплив УЗ, який різниться для низькотемпературної (НТ) області ($T < 180$ K) і високотемпературної (ВТ) ($T > 200$ K). У ВТ області акустостимульовані (АС) зміни незначні, дещо падає рухливість, довготривалі $\sigma(t)$ не проявляються. В НТ області відносні АС зміни зростають, збільшується тривалість релаксаційних процесів $\sigma(t)$, які проявляють двостадійний характер. Для пояснення використана модель неоднорідного напівпровідника, що містить кластери домішкових дефектів в околі дислокацій. Запропоновано механізм, який пов'язує "миттєві" зростання $\sigma(t)$ з АС зменшенням амплітуди флуктуацій крупномасштабного потенціалу в результаті збільшення ефективного електронного радіуса дислокаційних домішкових кластерів; довготривалі температурно-залежні релаксації (50–500 с) визначаються дифузійною перебудовою точково-дефектної структури в середині кластера, включаючи перебудову заряджених акцепторних комплексів $[(\mathrm{V}_{\mathrm{Cd}}^{2-}\mathrm{Cl}_{\mathrm{Te}}^{+})^{-}]$ в нейтральні – $[(\mathrm{V}_{\mathrm{Cd}}^{2-}2\mathrm{Cl}_{\mathrm{Te}}^{+})^{0}]$.